Acta Crystallographica Section B
Structural Science
ISSN 0108-7681

Ab initio structure determination of the high-temperature phase of anhydrous caffeine by X-ray powder diffraction

Patrick Derollez,* Natália T. Correia, Florence Danède, Frédéric Capet, Frédéric Affouard, Jacques Lefebvre and Marc Descamps

Laboratoire de Dynamique et Structure des Matériaux Moléculaires (UMR CNRS 8024), UFR de Physique, Bâtiment P5, Université des Sciences et Technologies de Lille, 59655 Villeneuve d'Ascq CEDEX, France

Correspondence e-mail: patrick.derollez@univ-lille1.fr

Received 26 November 2004
Accepted 18 February 2005

The high-temperature phase I of anhydrous caffeine was obtained by heating and annealing the purified commercial form II at 450 K. This phase I can be maintained at low temperature in a metastable state. A powder X-ray diffraction pattern was recorded at 278 K with a laboratory diffractometer equipped with an INEL curved position-sensitive detector CPS120. Phase I is dynamically orientationally disordered (the so-called plastic phase). The Rietveld refinements were achieved with rigid-body constraints. It was assumed that on each site, a molecule can adopt three preferential orientations with equal occupation probability. Under a deep undercooling of phase I, below 250 K, the metastable state enters in a glassy crystal state.

1. Introduction

Caffeine (1,3,7-trimethylpurine-2,6-dione, $C_8H_{10}N_4O_2$) is a common agrochemical and therapeutic agent. It is known to occur in a hydrated form and two anhydrous polymorphic varieties. The crystal structure of the hydrated form was determined a long time ago (Sutor, 1958) and confirmed recently (Edwards *et al.*, 1997). The existence of a fully ordered crystal phase for anhydrous caffeine was discussed (Griesser *et al.*, 1999; Carlucci & Gavezzotti, 2004). The physical characterization of the anhydrous states is really challenging because of the apparent impossibility of producing monophasic caffeine. Depending on the preparation and the history of the sample, a mixture of different forms was found (Müller & Griesser, 2003). The commercial form [designed by (II) in the following] transforms upon heating to form (I). Cesàro & Starec (1980) have shown a phase transformation at T_t = 426 K before the melting at T_m = 512 K and have suggested, on the basis of calorimetric studies, that the high-temperature phase I is structurally disordered. The crystal structure of phase I has not yet been solved. From X-ray powder diffraction measurements, different rhombohedral space groups have been proposed in which the molecules should be linked by very weak hydrogen bonds to form an ordered network (Edwards *et al.*, 1997). Stowasser & Lehmann (2002) suggest a monoclinic cell containing 20 molecules with a volume of 4450 Å^3.

In this paper we report the *ab initio* structure determination of the high-temperature phase I of caffeine from X-ray powder diffraction experiments. We show that this phase can be maintained at low temperature in the metastable state. A deep undercooling of phase I, below 250 K, transforms the metastable state into a glassy crystal state.

2. Experimental

Caffeine was purchased from Acros Organics. Before the experiments, commercial caffeine was purified by sublimation. The high-temperature phase I was obtained by heating the needle-shaped crystals in a sealed Lindemann glass capillary (ϕ = 0.7 mm) to approximately 450 K for approximately 15 min. The high-temperature phase was then quenched to 278 K by inserting the sample into a stream of nitrogen gas with fluctuations no larger than $\pm$ 0.1 K. Consequently, phase I was placed in a metastable situation and we checked that the evolution of the physical properties was too slow to be detected during the experiment. Near room temperature the transformation from phase I to phase II takes weeks or months (Epple *et al.*, 1995; Lehto & Laine, 1998).

The X-ray powder diffraction patterns were measured on a laboratory diffractometer equipped with an INEL curved, position-sensitive detector CPS120. A bent quartz monochromator selected the $K\alpha_1$ wavelength of a Cu X-ray tube (λ = 1.54056 Å). The sample was rotated during the experiments in order to reduce the effect of possible preferential orientations. The calibration of the detector was performed with an X-ray diffraction pattern of the standard compound $Na_2Ca_3Al_2F_{14}$ (NAC; Evain *et al.*, 1993). A cubic spline interpolation was performed between the Bragg peaks of NAC. Data were collected at 278 K with a total counting time of 15 h, in the 2θ range 0.3–114.7° (2θ step 0.029°). Diffraction patterns were also measured at different temperatures between 100 and 370 K to explore the phase diagram.

3. Results and discussion

The diffraction pattern of phase I at 278 K is shown in Fig. 1. In the whole angular range, less than 30 Bragg peaks, often with very low intensities, were observed. Therefore, we expect the existence of a high-symmetry crystallographic system. To determine the lattice parameters, 20 Bragg peaks in the angular range 10–60° (2θ) were fit with the program *N-Treor* (Altomare *et al.*, 2000). All the reflections were indexed with a hexagonal cell with the following parameters: a = 14.9404, c = 6.8997 Å; V = 1333.7 Å^3. The calculated figures of merit (de Wolff, 1968; Smith & Snyder, 1979) were: $M(20)$ = 76, $F(20)$ = 73 (0.0064, 43). Our lattice parameters were similar to the values proposed by Edwards *et al.* (1997).

The diffraction pattern from 10 to 70° (2θ) was refined using Le Bail's method (Le Bail *et al.*, 1988) of the program *FULLPROF* (Rodriguez-Carvajal, 2001; Roisnel & Rodriguez-Carvajal, 2002). A pseudo-Voigt function, a linear combination of a Lorentzian and a Gaussian of the same FWHM (full width at half maximum), was used to fit the Bragg peaks. This FWHM has a θ dependence according to Caglioti's law (Caglioti *et al.*, 1958). The asymmetry of the reflections was taken into account according to the Berar and Baldinozzi function (Bérar & Baldinozzi, 1993). The background was determined with a linear interpolation between 29 points regularly distributed from 10 to 70°.

The 39 refined parameters are as follows: the lattice parameters a and c, the zero-shift, the Caglioti profile parameters U, V, W, the mixing parameter η_0 of the pseudo-Voigt function and its 2θ-dependence X, two parameters for the asymmetry of the Bragg peaks and 29 points to define the background. The best estimated space group was determined with the help of the program *CHEKCELL* (Laugier & Bochu, 2001). This corresponds to the space group having the maximum checked reflections and the minimum calculated ones. The best space groups were found to be $R3c$ and $R\bar{3}c$. It is worthwhile noticing that neither of them correspond to the space group $R3$, which was proposed by Edwards *et al.* (1997). Consequently, Le Bail refinements were successively performed to test the two space groups $R3$ and $R3c$. The reliability factors obtained with these two groups are close. However, a careful visual inspection of the diffraction pattern and a detailed examination of the observed intensities provided by the refinements, showed that systematic extinctions due to the existence of a c-glide plane, *i.e.* the reflections ($h0l$), ($0kl$), ($00l$) with l odd, were not observable. These considerations unambiguously led to the possible space groups $R3c$ and $R\bar{3}c$. At the end of the Le Bail refinements with our space groups, the conventional reliability factors were R_p = 0.072, R_{wp} = 0.063, R_{exp} = 0.017, χ^2 = 13.4; the values of the lattice parameters were: a = 14.9376 (3), c = 6.8979 (1) Å, V = 1332.93 (5) Å^3. The widths of the

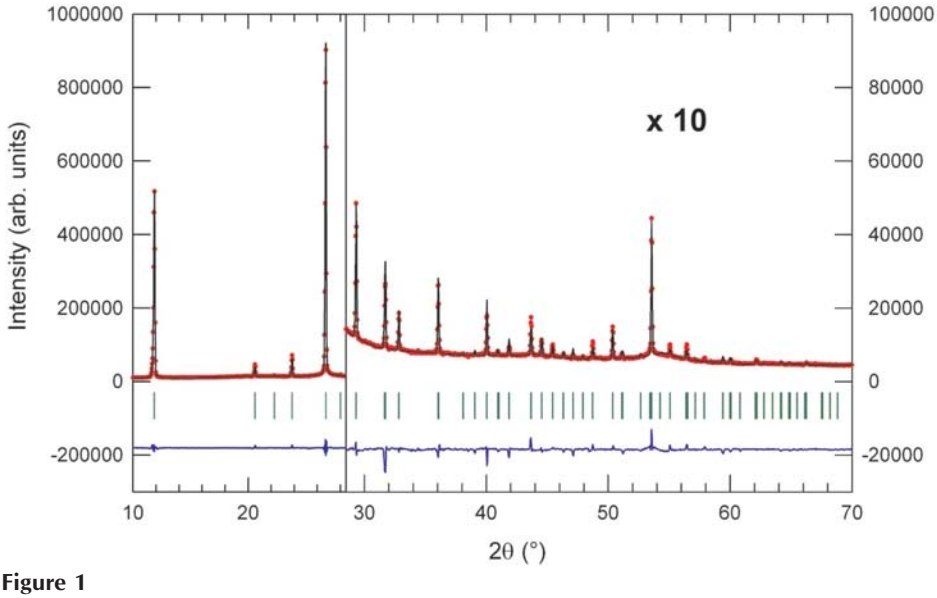

Figure 1
Final Rietveld plot of the high-temperature phase I of caffeine at 278 K. Observed intensities are indicated by dots, the best-fit profile (upper trace) and the difference pattern (lower trace) are solid lines. The vertical bars correspond to the positions of the Bragg peaks.

Table 1
Bond lengths (Å) in a molecule of caffeine for the Rietveld refinements.

C4—C5	1.349
C5—C6	1.430
C6—N1, N1—C2, C2—N3, N3—C4	1.394
C5—N7, N7—C8, C8—N9, N9—C4	1.345
N1—C10, N3—C12, N7—C14	1.478
O11—C2, O13—C6	1.217

Bragg peaks, close to the experimental resolution given by the NAC, do not allow a microstructural analysis (size of crystallites and micro-strain effects).

The density of caffeine, close to 1.45 g cm^{-3} (Edwards *et al.*, 1997), leads to a unit cell with six molecules. There are 18 symmetry equivalent positions for the space group $R3c$ and 36 for the group $R\bar{3}c$. This suggests the existence of an orientational disorder. The space group $R\bar{3}c$ is discarded because of the presence of the inversion centre. This would mean the possibility of a flip of the plane of the molecule. This eventuality appears unlikely and thus the dynamical disorder consists of a rotation of the molecule in its own plane. Therefore, the Rietveld refinements were achieved with the space group $R3c$. On each molecular site a molecule can adopt three preferential positions, each of them with an occupation factor equal to 1/3.

The dynamical origin of the molecular disorder is confirmed by dielectric relaxation spectroscopy. Fig. 2 shows the isochronal temperature dependence of the imaginary part of the dielectric permittivity when the sample is cooled from 425 K (phase I) to 220 K (metastable state, see below) for four representative frequencies. The existence of relaxational motions which are slower as the temperature is lowered are clearly shown. This indicates the thermally activated nature of this relaxation phenomenon. The dipolar relaxation time, close to 10^{-4} s at 400 K, is increased to 1 s at room temperature. It reaches 100 s at $T_g \simeq 250$ K (Descamps *et al.*, 2005). Below T_g, the dynamical disorder associated with the molecular rotations are frozen out and caffeine enters in a so-called glassy crystal state.

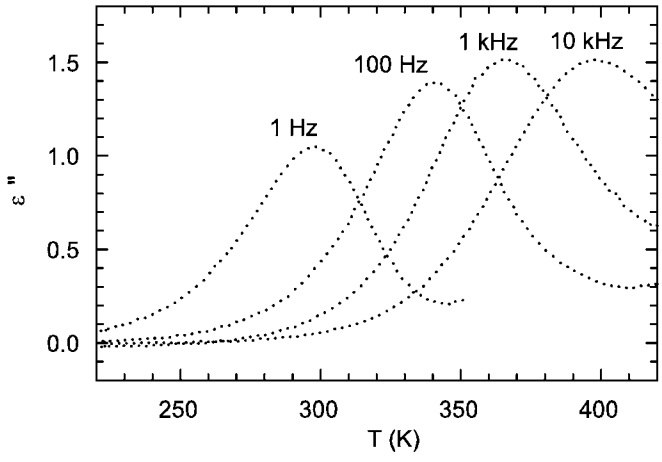

Figure 2
Isochronal temperature dependence of the imaginary part of the dielectric permittivity from dielectric relaxation spectroscopy.

Given the small number of (*hkl*) reflections (65 reflections in the range 10–70°) and the number of atomic coordinates to refine (14 non-H atoms × 3 coordinates), the molecule was taken as a rigid body and its geometry was built from the atomic coordinates of monohydrate caffeine (Edwards *et al.*, 1997), anhydrous theophylline (Ebisuzaki *et al.*, 1997), 1,7,9-trimethylpurine-2,6-dione monohydrate (Parvez, 1994) and from the complex of sulfacetamide–caffeine (Leger *et al.*, 1977). Fig. 3 shows a representation of the molecule drawn with *ORTEP*3 (Farrugia, 1997) and the numbering of the atoms. The bond lengths are reported in Table 1. The bond angles chosen were regular, the internal angles of the pyrimidine ring being equal to 120° and those of the imidazole ring equal to 108°. The position of the molecule in the asymmetric unit is thus defined by the determination of three Euler angles θ, φ and χ, which characterize the orientation of an orthonormal molecular system with respect to the orthonormal crystallographic system. The three parameters x_0, y_0 and z_0 represent the reduced coordinates of the centre of the rigid body (C4 atom) in the crystallographic system. The space group $R3c$ forces the coordinate z_0 to be fixed.

When plastic crystals are made up of nearly spherical molecules (CBr_4, C_{60}, adamantane, for example), the dynamical disorder consists of quasi-free rotations of the molecule around the centre of mass, while the translational order persists. For globular molecules, the plastic phase is often of cubic symmetry. When the molecules are flat, as in benzene derivatives, only axial rotations are released and the rotator phase is hexagonal (Brand *et al.*, 2002, and references therein). In the case of molecules with a quasi-circular disk structure, the rotation is easier around the axes perpendicular to the disk and the molecules preferentially lie in the hexagonal plane.

Therefore, for the first Rietveld refinements the plane of the molecule remained parallel to the hexagonal plane by fixing the angles θ and χ at the correct values and its centre of mass

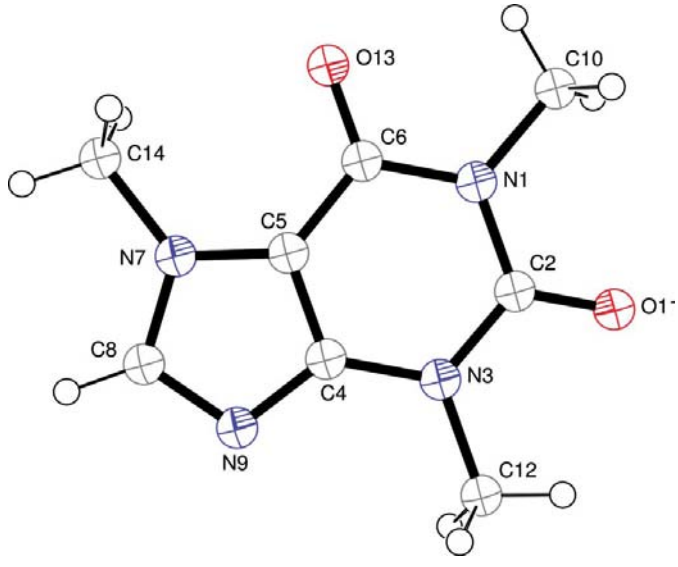

Figure 3
Atomic numbering and molecular structure of caffeine.

Table 2
Experimental data.

Crystal data	
Chemical formula	$C_8H_{10}N_4O_2$
M_r	194.20
Cell setting, space group	Trigonal, *R*3*c*
a, *b*, *c* (Å)	14.9372 (5), 14.9372 (5), 6.8980 (2)
V (Å^3)	1332.88 (7)
Z	6
D_c (Mg m^{-3})	1.452
F(000)	612
Radiation type	Cu *Kα*
μ (mm^{-1})	0.91
Temperature (K)	278
Specimen form, colour	Cylinder, white
Data collection	
Diffractometer	Inel CPS120
2θ (°)	$2\theta_{min}$ = 0.2928, $2\theta_{max}$ = 114.6978, increment = 0.029
Data collection method	Transmission
Refinement	
R factors and goodness-of-fit	R_p = 2.706, R_{wp} = 4.314, R_{exp} = 0.892, R_B = 2.256
Wavelength of incident radiation (Å)	1.540560
Excluded region(s)	0.2928–10, 70–114.6978
Profile function	Pseudo-Voigt
No. of parameters	47
$(\Delta/\sigma)_{max}$	< 0.0001
Preferred orientation correction	Marsh–Dollase function

Computer programs used: *FULLPROF* (Rodriguez-Carvajal, 2001).

was placed on the threefold axis. In the final refinements, there are 47 adjustable parameters:

(i) 10 profile parameters: the lattice parameters *a* and *c*, the zero-point, *U*, *V*, *W*, η_0 and *X* as defined above and two asymmetry parameters.

(ii) 8 structural parameters: the scale factor, the parameters which define the molecular orientation θ, φ, χ, x_0 and y_0, a parameter G_1 linked to the preferred orientations (March, 1932; Dollase, 1986) which were found along [0,0,1], and a global isotropic temperature factor B_{ov}.

(iii) 29 points to define the background.

The final conventional Rietveld factors are: R_p = 0.091, R_{wp} = 0.086, R_{exp} = 0.018, χ^2 = 23.4. The experimental and calculated diffraction patterns are shown in Fig. 1. Crystallographic data, profile and structural parameters are given in Table 2[1] and reduced coordinates for non-H atoms are given in Table 3.

The parameter G_1 = 0.836 (2) for the [001] preferred direction corresponds to a slightly needle-like habit of the crystallites. The overall temperature factor B_{ov} = 3.25 (18) Å^2 is consistent with the existence of a disordered phase. The plane of the molecules is practically parallel to the hexagonal plane, as shown in Fig. 4(*a*). The angle between the C5—C4 vector and the *c* axis is found to be equal to 91.28 (1)°, and the angle between the C2—C4 vector and the *c* axis is equal to 96.56 (1)°. The superposition of the three preferential orientations of the molecule is shown in Fig. 4(*b*) and an example of equilibrium positions in this hexagonal plane is given in Fig. 5. Given the dynamical disorder, the existence of an ordered network of hydrogen bonds seems to be impossible. A further attempt to refine the individual coordinates of the non-H atoms with soft restraints failed, as expected and explained above. The molecule becomes unrealistically distorted and non-planar.

The following two structural models were also tested independently: molecular conformation from monohydrate

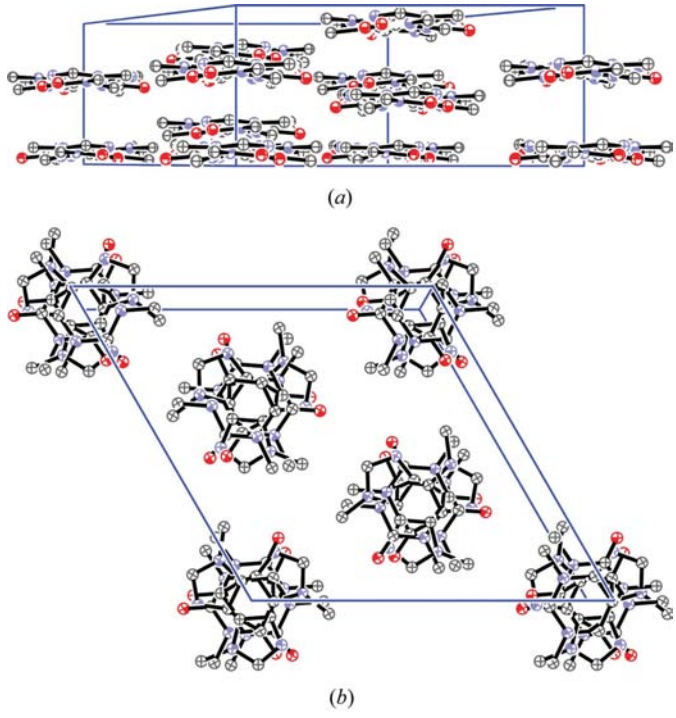

Figure 4
(*a*) Perspective drawing of the unit cell along the [100] direction. The molecules are nearly parallel to the hexagonal plane. (*b*) Perspective drawing of half a cell along the [001] direction showing the three preferential orientations of the molecule on each site.

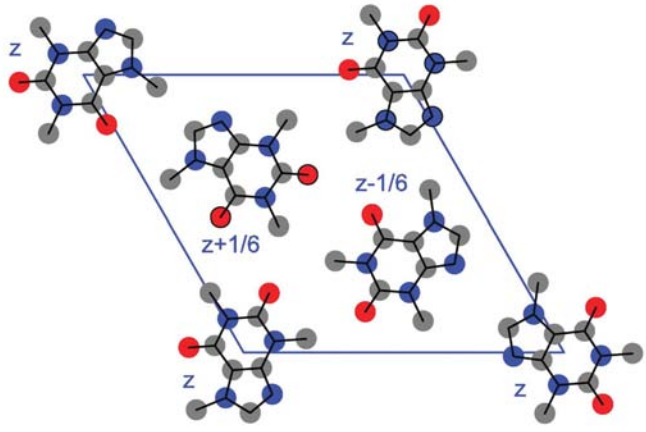

Figure 5
An example of equilibrium configurations in the hexagonal plane.

[1] Supplementary data for this paper are available from the IUCr electronic archives (Reference: LC5020). Services for accessing these data are described at the back of the journal.

Table 3
Reduced coordinates for non-H atoms.

The coordinates of the C4 atom coincide with the position x_0, y_0, z_0 of the rigid body.

C4	0.0278 (23)	−0.0553 (18)	0.1
C5	−0.0661	−0.0631	0.0956
N3	0.1168	0.0412	0.0823
C2	0.1087	0.1296	0.0600
O11	0.1863	0.2138	0.0445
N1	0.0116	0.1215	0.0555
C6	−0.0774	0.0250	0.0732
O13	−0.1621	0.0180	0.0692
N7	−0.1379	−0.1635	0.1155
N9	0.0139	−0.1509	0.1225
C8	−0.0886	−0.2178	0.1321
C14	−0.2511	−0.2066	0.1185
C12	0.2197	0.0497	0.0871
C10	0.0030	0.2153	0.0319

caffeine (Edwards *et al.*, 1997) and from the complex of sulfacetamide–caffeine (Leger *et al.*, 1977). The Rietveld refinements gave similar results (as an indication, R_p = 0.095, R_{wp} = 0.088 in the former case and R_p = 0.093, R_{wp} = 0.089 in the latter case), which can be compared with those obtained with our average molecule (R_p = 0.091, R_{wp} = 0.086). It appears that these similar results are a consequence of the weak dispersion of the bond lengths and bond angles in these substances.

The evolution of the diffraction pattern of undercooled phase I upon heating from 100 to 370 K is shown in Fig. 6. The overall hexagonal patterns remain unchanged. At 370 K, a strong decrease in some Bragg peak intensities appears. Simultaneously, the statistics become less well defined, indicating the beginning of the re-crystallization into the anhydrous stable phase II. No significant variations of the integrated intensities or of the widths of the Bragg peaks were

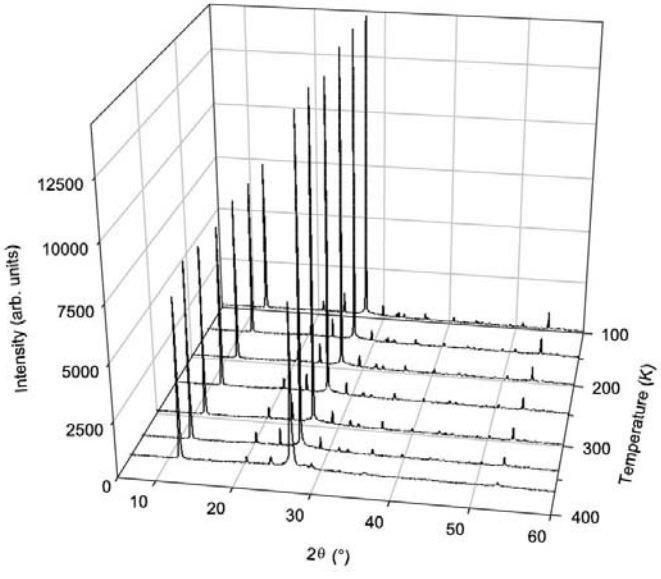

Figure 6
Selected powder patterns of the undercooled phase I at different temperatures.

Table 4
Linear and volume thermal expansion coefficients at 150 and 293 K.

$\times 10^{-5}$ K^{-1}	150 K	293 K
α_a	3.48	4.71
α_c	10.55	15.42
α_V	17.52	24.92

observed up to the transition. The lattice parameters were obtained by Le Bail refinements and their temperature dependence is shown in Fig. 7. Two distinct regimes are clearly shown. On both sides of 250 K, the variations are well fitted with straight lines. The linear and volume thermal expansion coefficients at 150 and 293 K are given in Table 4.

The jumps of the thermal expansion coefficients at 250 K are analogous to those observed in glass-forming liquids and

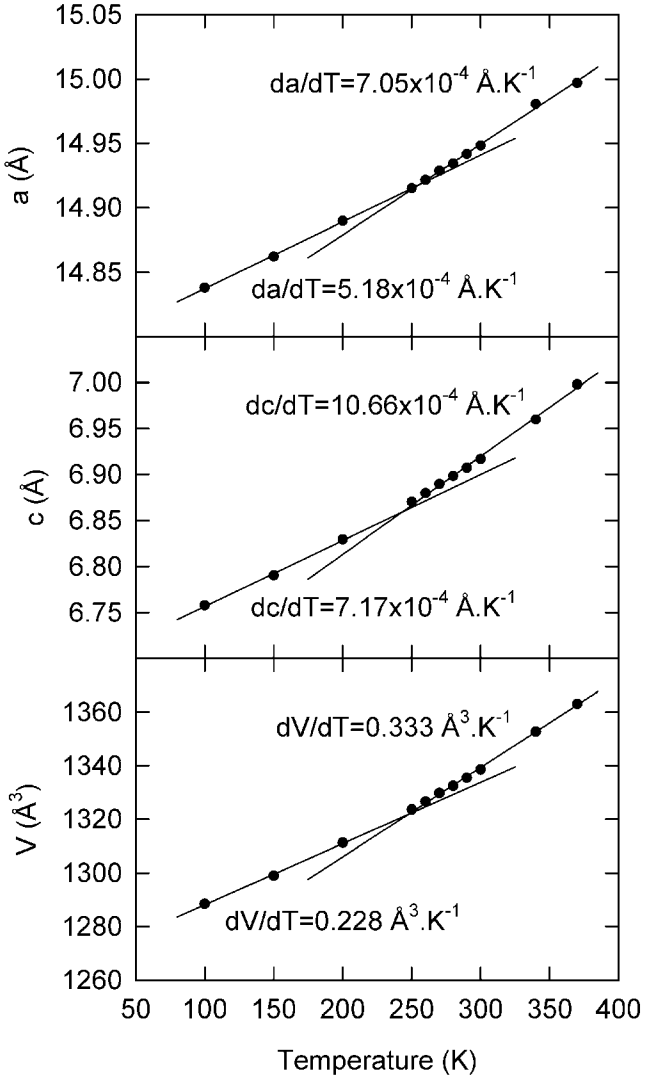

Figure 7
Lattice parameters and cell volume as functions of temperature. The dots represent the experimental data and the solids lines are fits as detailed in the text. The error bars are smaller than the dot size.

form a structural signature of the glass transition. From these X-ray diffraction and dielectric relaxation measurements we obtain the following picture: the high-temperature phase I is a dynamically, orientationally disordered crystalline phase between 250 and 370 K. Phase I can be easily supercooled, thus avoiding orientational ordering generally occurring at low temperatures. Below $T_g \simeq 250$ K, the orientational motions are frozen so that the orientational disorder can be considered as static, and the high symmetry phase is kept in a glassy crystal state. These conclusions are corroborated by calorimetric and dielectric studies (Descamps *et al.*, 2005).

The authors thank Professor A. Cesàro and Professor U. Griesser for fruitful discussions and Professor A. Gavezzotti for communicating his results before publication. N. T. Correia acknowledges a post-doctoral grant from the *Fundação para a Ciência e Tecnologia*. This work has been made in the framework of the program INTERRREG III 'thema' supported by the FEDER.

References

Altomare, A., Giacovazzo, C., Guagliardi, A., Moliterni, A. G. G., Rizzi, R. & Werner, P. E. (2000). *J. Appl. Cryst.* **33**, 1180–1186.
Bérar, J. F. & Baldinozzi, G. (1993). *J. Appl. Cryst.* **26**, 128–129.
Brand, R., Lunkenheimer, P. & Loidl, A. (2002). *J. Chem. Phys.* **116**, 10386–10401.
Caglioti, G., Paoletti, A. & Ricci, F. P. (1958). *Nucl. Instrum.* **3**, 223–228.
Carlucci, L. & Gavezzotti, A. (2004). Personal communication.
Cesàro, A. & Starec, G. (1980). *J. Phys. Chem.* **84**, 1345–1346.
Descamps, M., Correia, N. T., Derollez, P., Danède, F. & Capet, F. (2005). Accepted for publication.
Dollase, W. A. (1986). *J. Appl. Cryst.* **19**, 267–272.
Ebisuzaki, Y., Boyle, P. D. & Smith, J. A. (1997). *Acta Cryst.* C**53**, 777–779.
Edwards, H. G. M., Lawson, E., Matas, M. de, Shields, L. & York, P. (1997). *J. Chem. Soc. Perkin Trans. 2*, pp. 1985–1990.
Epple, M., Cammenga, H. K., Sarge, S. M., Diedrich, R. & Balek, V. (1995). *Thermochim. Acta*, **250**, 29–39.
Evain, M., Deniard, P., Jouanneaux, A. & Brec, R. (1993). *J. Appl. Cryst.* **26**, 563–569.
Farrugia, L. (1997). *J. Appl. Cryst.* **30**, 565.
Griesser, U. J., Szelagiewicz, M., Hofmeier, U. ch., Pitt, C. & Cianferani, S. (1999). *J. Thermal Anal. Calorim.* **57**, 45–60.
Laugier, J. & Bochu, B. (2001). *CHEKCELL*; http://www.inpg.Fr/LMGP.
Le Bail, A., Duroy, H. & Fourquet, J. L. (1988). *Mater. Res. Bull.* **23**, 447–452.
Leger, J.-M., Alberola, S. & Carpy, A. (1977). *Acta Cryst.* B**33**, 1455–1459.
Lehto, V.-P. & Laine, E. (1998). *Thermochim. Acta*, **317**, 47–58.
March, A. (1932). *Z. Kristallogr.* **81**, 285–297.
Müller, P. R & Griesser, U. J. (2003). *PhandTA7, 7th Int. Conf./Workshop on Pharmacy and Applied Physical Chemistry*, 7–11 September, Innsbruck, Austria.
Parvez, M. (1994). *Acta Cryst.* C**50**, 1303–1305.
Rodriguez-Carvajal, J. (2001). *FULLPROF*, Version 1.9c. LLB, CEA/Saclay, France.
Roisnel, T. & Rodriguez-Carvajal, J. (2002). *Mater. Sci. Forum*, **378–381**, 118–123.
Smith, G. S. & Snyder, R. L. (1979). *J. Appl. Cryst.* **12**, 60–65.
Stowasser, F. & Lehmann, C. (2002). *Acta Cryst.* A**58**, C265.
Sutor, D. J. (1958). *Acta Cryst.* **11**, 453–458.
Wolff, P. M. de (1968). *J. Appl. Cryst.* **1**, 108–113.